Trojan horse particle invariance studied with the ^{6}Li(d,α)^{4}He and ^{7}Li(p,α)^{4}He reactions

R. G. Pizzone,[1] C. Spitaleri,[1,2] L. Lamia,[1,2] C. Bertulani,[3] A. Mukhamedzhanov,[4] L. Blokhintsev,[5] V. Burjan,[6] S. Cherubini,[1,2] Z. Hons,[6] G. G. Kiss,[1,7] V. Kroha,[6] M. La Cognata,[1,2] C. Li,[8] J. Mrazek,[6] Š. Piskoř,[6] S. M. R. Puglia,[1,2] G. G. Rapisarda,[1,2] S. Romano,[1,2] M. L. Sergi,[1,2] and A. Tumino[1,9]

[1]*Laboratori Nazionali del Sud-INFN, Catania, Italy*
[2]*Dipartimento di Fisica e Astronomia, Università di Catania, Catania, Italy*
[3]*Department of Physics and Astronomy, Texas A&M University-Commerce, Commerce, Texas 75025, USA*
[4]*Cyclotron Institute, Texas A&M University, College Station, Texas, USA*
[5]*Institute of Nuclear Physics, Moscow State University, Moscow, Russia*
[6]*Institute of Nuclear Physics of ASCR, Praha-Řež, Czech Republic*
[7]*Atomki, Debrecen, Hungary*
[8]*Beijing Radiation Center, Beijing, China*
[9]*Università degli Studi di Enna "Kore," Enna, Italy*

(Received 11 January 2011; revised manuscript received 4 March 2011; published 11 April 2011)

The Trojan horse nucleus invariance for the binary reaction cross section extracted from the Trojan horse reaction was tested using the quasifree ^{3}He(^{6}Li,$\alpha\alpha$)H and ^{3}He(^{7}Li,$\alpha\alpha$)^{2}H reactions. The cross sections for the ^{6}Li(d,α)^{4}He and ^{7}Li(p,α)^{4}He binary processes were extracted in the framework of the plane wave approximation. They are compared with direct behaviors as well as with cross sections extracted from previous indirect investigations of the same binary reactions using deuteron as the Trojan horse nucleus instead of ^{3}He. The very good agreement confirms the applicability of the plane wave approximation which suggests the independence of the binary indirect cross section on the chosen Trojan horse nucleus, at least for the investigated cases.

DOI: 10.1103/PhysRevC.83.045801 PACS number(s): 25.60.Pj, 21.10.Pc, 24.50.+g, 25.55.Hp

I. INTRODUCTION

The study of nuclear reactions induced by charged particles at astrophysical energies has many experimental difficulties, mainly connected to the presence of the Coulomb barrier and the electron screening effect. For these reasons several indirect methods have been developed, mainly based on direct reactions. Among them, an important role is played by the Trojan horse method (THM). It has been applied to several reactions in the past decade [1–12] at the energies relevant for astrophysical applications, which usually are far below the Coulomb barrier. In recent years many tests have been made to deepen the knowledge of the method and extend its possible applications: the target-projectile breakup invariance [13], the spectator invariance [14], and the possible application to neutron beams [15,16]. Such studies are crucial, as the Trojan horse method has become one of the major tools for the investigation of reactions of astrophysical interest (for a recent review see, e.g., [17]). In a recent work [14] a test TH nucleus invariance was performed for the ^{7}Li(d,$\alpha\alpha$)n and the ^{7}Li(^{3}He,$\alpha\alpha$)^{2}H reactions, thus comparing results from deuteron and ^{3}He targets. In Ref. [14] the ^{7}Li(p,α)^{4}He two-body cross section was deduced in the PW approach using only a part of the collected experimental data, and compared with the direct behavior as well as with previous indirect data from the ^{7}Li(d,$\alpha\alpha$)n reaction [18]. Agreement between the sets of data was found below and above the Coulomb barrier. This suggests that ^{3}He is a good "Trojan horse nucleus," in spite of its quite high ^{3}He$\rightarrow d + p$ breakup energy (5.49 MeV), and that the THM cross section does not depend on the chosen Trojan horse nucleus, at least for the ^{7}Li-p interaction.

The present paper will be devoted to the investigation of the TH nucleus invariance for the ^{6}Li(d,α)^{4}He case at energies above and below the ^{6}Li-d Coulomb barrier and to the reanalysis of the ^{7}Li(p,α)^{4}He reaction using all available experimental data. Our aim is to show that in both cases the plane wave approximation (PWA) is valid and that the use of a different spectator particle does not influence the THM reliability, at least for the examined cases.

II. TROJAN HORSE METHOD

The Trojan horse method (THM) allows one to extract the low energy behavior of an astrophysically relevant binary reaction by applying the well known theoretical formalism of the quasifree (QF) process. Both the THM and QF process are direct mechanisms in which the interaction between an impinging nucleus and the target can cause the breakup of the target (TBU) or of the projectile (PBU) (see a schematic description in Fig. 1). In particular, these processes have three particles in the exit channel, one of which can be thought as a spectator to the binary interaction of interest. In the case of TBU and referring to Fig. 1, the assumption is that of an interaction between the impinging nucleus a and one of the clusters constituting the target (called participant, x), while the residual nucleus, s, does not participate in the reaction. The spectator s is free from any effect due to the interaction between the incoming nucleus and the participants, reflecting in the exit channel the same momentum distribution for the intercluster (xs) motion inside b it had before the occurrence of the QF breakup.

The basic idea of the THM [19] is to extract the cross section of an astrophysically relevant two-body reaction

$$a + x \rightarrow c + C \qquad (1)$$

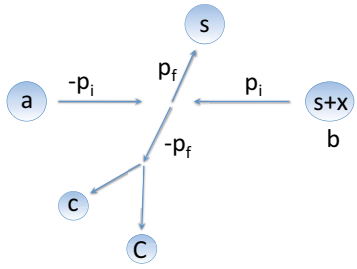

FIG. 1. (Color online) Schematic representation of a three-body (in the final channel) reaction used in the Trojan horse method.

at low energies from a suitable three-body QF reaction (see Figs. 1 and 2),

$$a + b \rightarrow s + c + C. \tag{2}$$

Under appropriate kinematical conditions, the three-body reaction $a(b, cC)s$ is considered as the decay of the "Trojan horse" b into the clusters x and s followed by the interaction of a with x. If the bombarding energy E_a is chosen high enough to overcome the Coulomb barrier in the entrance channel of the reaction, the effect of the Coulomb barrier and electron screening effects are negligible.

Application of the THM significantly simplifies if the PWA is valid. In the PWA the triple differential cross section in the center of mass of the TH reaction can be written as

$$\frac{d^3\sigma^{\mathrm{TH}}}{dE_{cC}d\Omega_{cC}d\Omega_{sF}} = \lambda^{(3)} \left|I^b_{sx}(\mathbf{k}_{sx})\right|^2 |M(\mathbf{k}_{xa},\ \mathbf{p}_{cC})|^2, \tag{3}$$

where

$$\lambda^{(3)}_3 = \frac{\mu_{ab}\,\mu_{sF}\,\mu_{cC}}{2\,\pi^5}\,\frac{p_{sF}\,p_{cC}}{p_{ab}} \tag{4}$$

is the kinematical factor for the triple differential cross section, $I^b_{sx}(\mathbf{k}_{sx})$ is the Fourier transform of the overlap function of the bound state wave functions of nuclei b, s, and x, $\mathbf{p}_{ij}$ is the relative momentum of the real (on-the-energy-shell) particles, $\mathbf{k}_{ij}$ is the relative momentum of particles i and j when one (or both particles) is virtual (off-the-energy-shell), E_{ij} and μ_{ij} are the relative kinetic energy and the reduced mass of particles i and j, Ω_{ij} is the solid angle between particles i and j, and $F = a + x = c + C$. $M(\mathbf{k}_{xa},\ \mathbf{p}_{cC})$ is the reaction

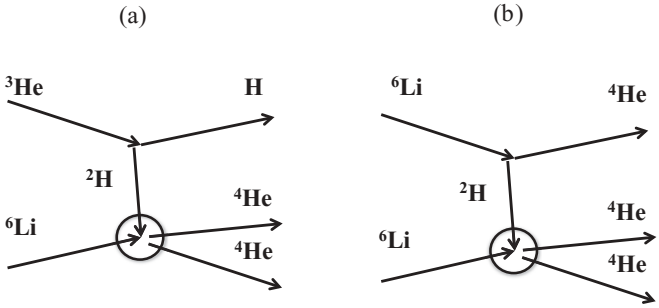

FIG. 2. (a) Diagram describing the QF mechanism in the case of ^{3}He breakup. (b) Diagram describing the QF mechanism in the case of ^{6}Li breakup.

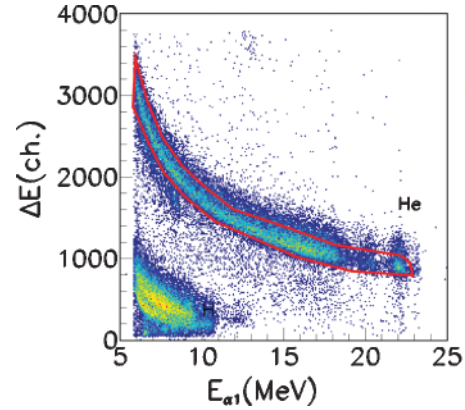

FIG. 3. (Color online) $\Delta E/E$ matrix for telescope T1 with the experimental cut for ^{3}He adopted for the present analysis.

amplitude, which describes the binary subreaction (1) with virtual particle x in the entry channel of the reaction. Hence we can call $M(\mathbf{k}_{xa}, \mathbf{p}_{cC})$ the half-off-energy-shell (HOES) reaction amplitude. As a scalar function, $M(\mathbf{k}_{xa}, \mathbf{p}_{cC})$, in contrast to the on-the-energy-shell binary reaction amplitude, due to the virtual character of x, depends on three kinematical invariants k_{xa}, p_{cC}, and $\hat{\mathbf{k}}_{xa} \cdot \hat{\mathbf{p}}_{cC}$. Here, $\hat{\mathbf{p}} = \mathbf{p}/p$. However, it can be shown that in the QF kinematics k_{ax} can be expressed in terms of p_{cC}; i.e., in the QF kinematics $M(\mathbf{k}_{xa}, \mathbf{p}_{cC})$ depends, as the on-shell binary reaction amplitude, only on two kinematical invariants. To show this we take into account that in the PWA [9]

$$E_{ax} = \frac{k^2_{ax}}{2\,\mu_{ax}} - \frac{k^2_{sx}}{2\,\mu_{sx}} - \varepsilon_{sx}. \tag{5}$$

Here, ε_{sx} is the binding energy of b for the virtual decay $b \rightarrow s + x$. Thus, in the TH reaction always $p_{ax} = \sqrt{2\,\mu_{ax}\,E_{ax}} < k_{ax}$. In the QF kinematics, $k_{sx} = 0$, and Eq. (5) reduces to

$$E_{ax} = \frac{k^2_{ax}}{2\,\mu_{ax}} - \varepsilon_{sx}. \tag{6}$$

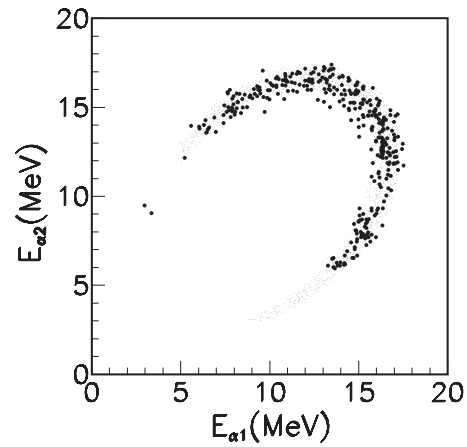

FIG. 4. Experimental kinematic locus (solid thick circles) for $\theta_{\alpha 1} = 70^\circ \pm 1^\circ$ and $\theta_{\alpha 2} = 70^\circ \pm 1^\circ$ superimposed onto the result of a simulation (thinner circles) as discussed in the text.

But E_{ax} and $E_{cC} = p_{cC}^2/(2\,\mu_{cC})$ are connected by the energy conservation $E_{ax} + Q_2 = E_{cC}$, where $Q_2 = m_a + m_x - m_c - m_C$. Thus in the QF kinematics one can express k_{ax} in terms of k_{cC}. Hence, in the QF the amplitude of the HOES binary reaction $M(\mathbf{k}_{xa}, \mathbf{p}_{cC})$ depends only two independent variables p_{cC} and $\hat{\mathbf{k}}_{xa} \cdot \hat{\mathbf{p}}_{cC}$.

The success of THM relies on the QF kinematics (equivalent to $p_s \sim 0$ for nuclei such as ^{3}He or ^{2}H), at which the TH conditions are best fulfilled. The occurrence of the QF mechanism at low energies has been pointed out in a number of works [18]. We will see how by applying the conditions on the momentum distribution of the spectator, as discussed in Ref. [20], we can use the quite simple PW. This was already observed for the first time in Ref. [21]. It has also been verified that for spectator momenta around zero the PW gives results similar to those obtained by more complicate approaches, as reported in Ref. [22].

Now we can introduce the HOES two-body differential cross section for the binary reaction (1),

$$\frac{d\sigma^{\mathrm{HOES}}_{a+x\to c+C}}{d\Omega_{cC}} = \lambda^{(2)}\,|M(\mathbf{k}_{xa},\ \mathbf{p}_{cC})|^2, \tag{7}$$

where

$$\lambda_2 = \frac{\mu_{ax}\,\mu_{cC}}{4\,\pi^2}\,\frac{p_{cC}}{p_{ax}} \tag{8}$$

is the kinematical factor. It is important to underline that we have a degree of freedom when defining the HOES differential cross section because the entry channel is off the energy shell; i.e., we can use as the entry momentum k_{ax} or p_{ax}. In Eq. (7) we use the latter. Then the TH triple differential cross section can be written in a factorized form in terms of the HOES differential cross section whose energy trend is the point of interest for the THM. Its absolute value can be extracted through normalization to the direct data available at higher energies,

$$\frac{d^3\sigma^{\mathrm{TH}}}{dE_{cC}d\Omega_{s_F}d\Omega_{cC}} = \frac{\lambda_3}{\lambda_2}\left|I^b_{sx}(\mathbf{k}_{sx})\right|^2\frac{d\sigma^{\mathrm{HOES}}_{a+x\to c+C}}{d\Omega_{cC}}. \tag{9}$$

Thus, if the PW is valid, the HOES differential cross section for the binary subreaction determined from the TH reaction does not depend on the type of the TH nucleus $b = (sx)$:

$$\frac{d\sigma^{\mathrm{HOES}}_{a+x\to c+C}}{d\Omega_{cC}} = \frac{\lambda_2}{\lambda_3}\,\frac{1}{\left|I^b_{sx}(\mathbf{k}_{sx})\right|^2}\,\frac{d^3\sigma^{\mathrm{TH}}}{dE_{cC}d\Omega_{s_F}d\Omega_{cC}}. \tag{10}$$

This independence of the HOES differential cross section extracted from the TH reaction on the type of the TH nucleus is called TH nucleus invariance of the HOES cross section. This means that the study of a binary reaction of astrophysical interest, $a(x, c)C$, via a QF process with three particles in the exit channel, can proceed whatever the spectator particle is. Hence, instead of studying the binary reaction through the $a(b, cC)s$ reaction, one can study it by means of the $a(b', cC)s'$ reaction, as can be seen by comparing the lower part of the two diagrams in Fig. 2, for example. This represents the invariance of the lower vertex describing the binary subreaction amplitude with respect to changes in the upper one (breakup of Trojan horse nucleus).

TABLE I. Experimental details of the setup described in the text.

Detector	Distance (mm)	Angular Range (deg)
PSD1	210	63–77
PSD2	210	23–37
PSD3	210	63–77
PSD4	210	113–127

III. THE EXPERIMENT

The present experiment was aimed at studying the ^{6}Li(d,α)^{4}He reaction by means of the THM applied to the ^{6}Li(^{3}He,$\alpha\alpha$)H three-body reaction. The experiment was performed at the Nuclear Physics Institute, Nuclear Reactions Department of the ASCR in Řež (Praha). The isochronous cyclotron provided a 17.5 MeV ^{3}He beam with intensity of 2 enA with a diameter of about 2 mm on target. The isotopically enriched ^{6}LiF target of about 280 μg/cm^2 was placed with its normal parallel to the beam axis. The experimental setup aiming to detect the two alpha particles consisted of four 50×10 mm^2 position-sensitive detectors (PSDs). For particle identification two 450 mm^2 25 μm thick Ametek silicon detectors were placed in front of two different PSDs as the ΔE step of a standard $\Delta E/E$ telescope. The angular positions of such detectors were chosen in order to cover the largest part of the kinematic conditions where a strong QF contribution is expected, i.e., to cover the angular regions corresponding to low momenta of the third, undetected particle (in our case a proton). The experimental features of the setup are summarized in Table I. The choice of such angular ranges is crucial for the following analysis via the THM, since they were chosen within the QF angular pairs. The signals of each detector were processed by a standard electronic chain which provided also the experiment trigger defined by the PSD1-PSD3 and PSD2-PSD4 coincidences (logical OR).

IV. DATA ANALYSIS

The detectors used in the experimental run were calibrated both in energy and position. Standard reactions and scatterings of the 17.5 MeV ^{3}He beam with a gold and carbon target were used in the preliminary calibration runs as well as alpha source. The angular calibration was performed by means of a grid, placed in front of each detector. The angular positions of each slit in the grids was measured by means of optical methods with a spatial resolution of about 0.2°.

The first step of the analysis is to discriminate the three-body reaction of interest from all the others induced by the interaction of the ^{3}He beam with the LiF target. Using the standard $\Delta E/E$ technique (see Fig. 3), it was possible to select the alpha particles in the telescope detector while no identification of the other alpha particle was needed since the high Q-value ($Q_3 = 16.87$ MeV) in the exit channel assures a good separation from the other possible exit channels. The scatter plot of the detected alpha-particle energies, i.e., the so-called kinematical locus (Fig. 4), for the selected events was studied and it turned out to be in agreement with our simulations. Since the experimental setup was conceived in

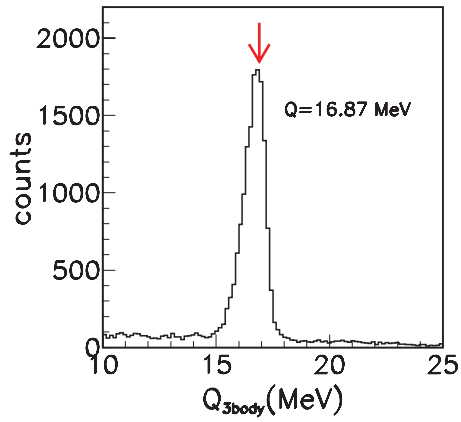

FIG. 5. (Color online) Q-value spectrum for the ^{6}Li(^{3}He,$\alpha\alpha$)H reaction. The theoretical value is around 16.87 MeV.

order to allow for a complete kinematic reconstruction, under the hypotheses that the third undetected particle has mass number 1, all the variables of interest were calculated. By means of energy conservation, the Q-value spectrum for the selected events was reconstructed and is given in Fig. 5. The position of a well separated peak is compared with the theoretical Q value of 16.87 MeV for the ^{6}Li(^{3}He,$\alpha\alpha$)H reaction. The agreement, within the experimental uncertainties, is a signature of our good calibration and a precise selection of the three-body channel. Only the events falling inside the Q-value peak, arising from the ^{6}Li(^{3}He,$\alpha\alpha$)H reaction, are taken in account in the following sections.

V. IDENTIFICATION OF THE QF CONTRIBUTION

The next step of the THM data analysis is the study of the reaction mechanisms feeding the exit channel. This is a necessary stage to disentangle the QF events from those ascribed to other mechanisms producing the same ejectiles in the final state. In particular, for our case, the study of the $E_{\alpha\alpha}$, $E_{\alpha p}$, and $E_{\alpha p}$ relative energies allows one to obtain information on the presence of excited states of ^{8}Be and ^{5}Li, respectively. From such analysis different states of ^{8}Be

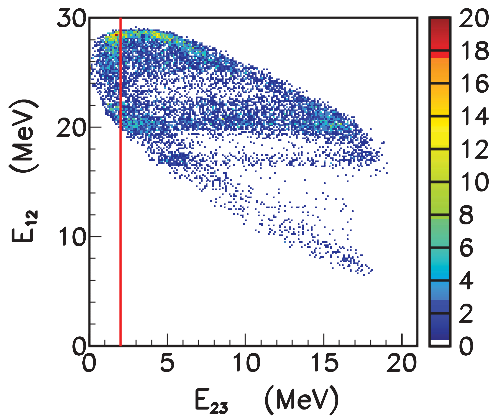

FIG. 6. (Color online) Relative energy two-dimensional plot. The level associated with ^{5}Li is marked with a red line.

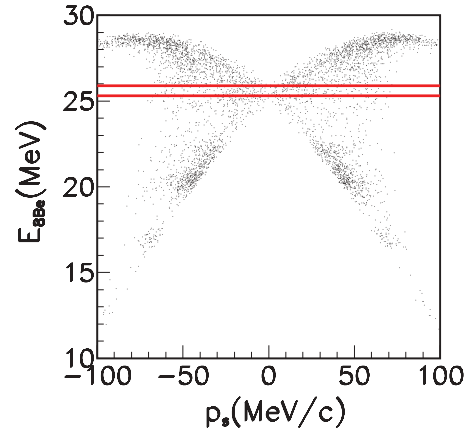

FIG. 7. (Color online) Relative energy vs p_s two-dimensional plot for $\theta_{cm} = 90^\circ \pm 5^\circ$. The red box shows the narrow energy cut adopted.

are recognized as horizontal loci in Fig. 6. In particular the contribution of the 25.2 MeV ($J^\pi = 2^+$) state corresponding to a $l = 2$ resonance in the ^{6}Li-d system at 2.8 MeV must be carefully evaluated. A contribution at about 1.7 MeV in the α-p relative energies, E_{23}, can be attributed to the presence of the ground state of the ^{5}Li. This last contribution is clearly related to sequential mechanism for which the formation of ^{5}Li produces in the exit channel the same particles of interest for our application (α, α, and p). Such mechanism causes then a background for the experimental data and should be removed before proceeding to further analysis. Moreover according to [23] the final state interaction (FSI) is relevant for E_{23} (or equivalently E_{13}) around 1.9 MeV. For this reason and in order to discard the sequential mechanism shown above, we restricted our analysis only to data with both E_{13} and E_{23} larger than 2.5 MeV, thus ensuring that the sequential decays are not present and that FSI contribution in the following analysis is negligible.

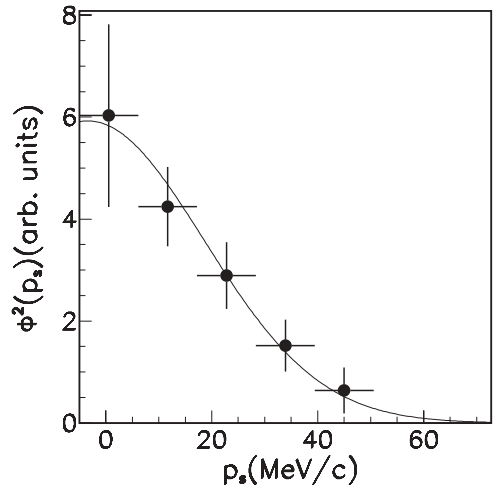

FIG. 8. Momentum distribution for p inside ^{3}He obtained as reported in the text. The FWHM is about 62 ± 6 MeV/c.

A. Evidence for QF mechanism

Among all the available observables, the most sensitive to the involved reaction mechanisms is the shape of the momentum distribution $|\varphi(\mathbf{p}_s)|^2$. Thus, the tests to discriminate the QF contribution from all the others are based on the study of this quantity. In order to extract the experimental momentum distribution of the spectator, $|\varphi(\mathbf{p}_s)|^2_{\rm exp}$, the energy sharing method can be applied to each pair of coincidence detectors, selecting narrow energy and angular windows, $\Delta E_{\rm cm}$ and $\Delta\theta_{\rm cm}$. The center-of-mass angle $\theta_{\rm cm}$ is defined following [24]. The $E_{\rm cm}$ cut, $\Delta E_{\rm cm} = 100$ keV, is displayed in the $E_{\rm cm}$ vs p_s 2D spectrum for $\theta_{\rm cm} = 90^\circ \pm 5^\circ$ (Fig. 7).

Keeping in mind the factorization of Eq. (10), since $[(d\sigma/d\Omega)_{\rm cm}]^{\rm HOES}$ is nearly constant in a narrow energy and $\theta_{\rm cm}$ window, one can get the shape of the momentum distribution of the undetected proton directly from the coincidence yield divided by the kinematical factor. After this test we can stress the role of the proton as a spectator to the QF process. The obtained momentum distribution for proton in ^{3}He is shown in Fig. 8. The solid line reported in the figure represents the Fourier transform of the Eckart function with a FWHM of about 62 ± 6 MeV/c, thus confirming the presence of the QF mechanism. This result is consistent with what has been observed for the ^{3}He nucleus in [25,26] as regards the correlation between the transferred momentum ($q_t \simeq 250$ MeV/c in the present case) and the width at half maximum of the experimental momentum distribution (see Fig. 9 for clearness). According to the prescription adopted in [20], data in the $|p_s| <$ 35 MeV/c range were chosen and used in the further analysis.

The results were compared with recent results [25,26] on distortion effects in reactions induced by light nuclei. The expected FWHM of the p momentum distribution in ^{3}He is around 64 ± 5 MeV/c. In Fig. 9 the good agreement of these results (black dots) is shown thus confirming what was observed for ^{3}He in [25,26] (solid line).

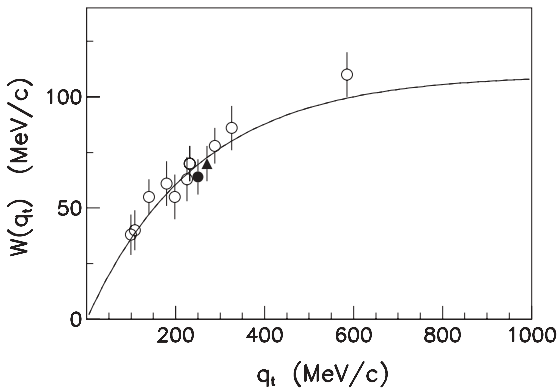

FIG. 9. Full width of the momentum distribution for p inside ^{3}He obtained as reported in the text compared with the behavior (solid line) and data (open circles) reported in [25,26]. Results from present data are shown as a filled circle for the ^{6}Li(^{3}He,$\alpha\alpha$)H and filled triangle for the ^{7}Li(^{3}He,$\alpha\alpha$)^{2}H reaction (see Sec. VII). A nice agreement is evident.

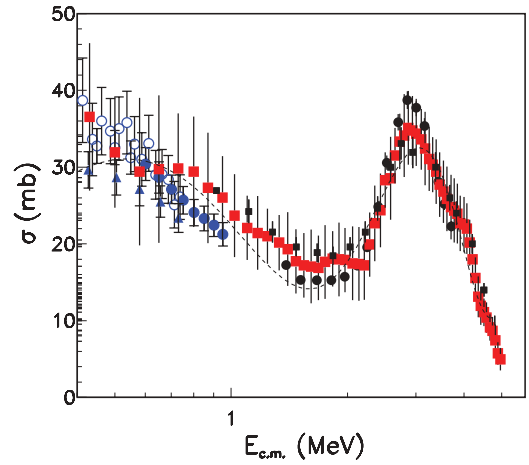

FIG. 10. (Color online) Excitation function for the ^{6}Li(d,α)^{4}He reaction extracted by means of THM. The indirect data (red squares) are normalized and compared with direct ones from [28] (black dots), [29] (black squares), [31] (blue circles), and [32] (triangles). The agreement is clearly evident both below and above the Coulomb barrier.

VI. RESULTS

In the standard THM analysis, the two-body cross section [Eq. (10)] is derived by dividing the experimental three-body one by the product $(\lambda_3/\lambda_2)\,|I^b_{sx}(\mathbf{p}_{sx})|^2$ (which is calculated by means of a Monte Carlo simulation). The width of the momentum distribution was set to the experimentally measured value in order to account for the distortion effects arising at low transferred momenta [26]. The first validity check that standard THM prescriptions do recommend is to reproduce the direct excitation function both below and above the Coulomb barrier. This is done by comparing the distributions measured with direct methods to the one measured by means of THM. The latter should be normalized to the direct data.

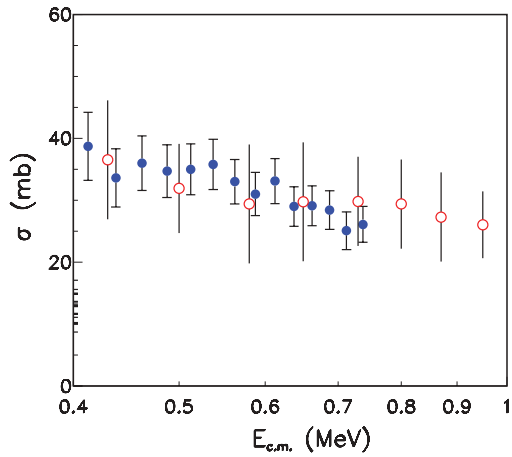

FIG. 11. (Color online) Excitation function for the ^{6}Li(d,α)^{4}He reaction extracted by means of THM. The present data (red circles) are compared with the ones extracted from the ^{6}Li breakup (blue circles [3]). The TH nucleus invariance test is clearly fulfilled. The two data sets were normalized to direct data separately.

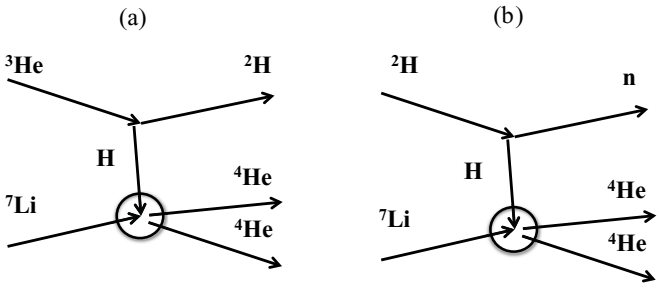

FIG. 12. Different breakup schemes adopted for studying the ^{7}Li(p,α)^{4}He reaction. In (a) the process is studied after ^{3}He breakup while in (b) after deuteron breakup.

The THM cross section is corrected for the penetrability factor (below the Coulomb barrier) which also make it possible the comparison of half-of-shell and on-shell data [27]. The penetrability factor is, as usual, described in terms of the regular and irregular Coulomb functions [3]. In particular, due to the presence of the $l = 2$ resonant state in the entrance ^{6}Li-d channel, a function describing the nonresonant $l = 0$ term as well as one describing the $l = 2$ term was taken into account to get the THM data. For each contribution two different normalization coefficients were determined by comparison with the direct data (following the same procedure reported in [6]).

The measured cross section, extracted by the THM, is compared, after normalization, in the $E_{cm} = 0.4$–5 MeV energy range with several data sets present in the literature [28–31] (Fig. 10). The agreement is very good throughout the whole energy range after normalization of the indirect to direct data. Moreover the resonance at about 3 MeV (corresponding to the 25.2 MeV, 2^+, energy level in ^{8}Be) is clearly reproduced.

The investigation of this energy range is not relevant for astrophysical implications for the ^{6}Li depletion [33] but it provides a strong validity test for THM. In fact, as in [6], the excitation function extracted in an indirect way does indeed reproduce the direct data both below and above the Coulomb barrier. Another interesting aspect of this analysis is the possibility of studying the TH nucleus invariance of the QF mechanism [14]. It is assumed, in fact, that changing the spectator particle in the QF process (on which is founded the THM) does not give any change to the binary reaction of interest. If we zoom in on the energy range 0.4–1 MeV in the present data, we can compare data for the ^{6}Li(d,α)^{4}He arising from the ^{6}Li(^{3}He,$\alpha\alpha$)H reaction (present work) with the ones extracted from ^{6}Li(^{6}Li,$\alpha\alpha$)^{4}He [3,13] (see Fig. 11). The agreement is very good within the experimental errors.

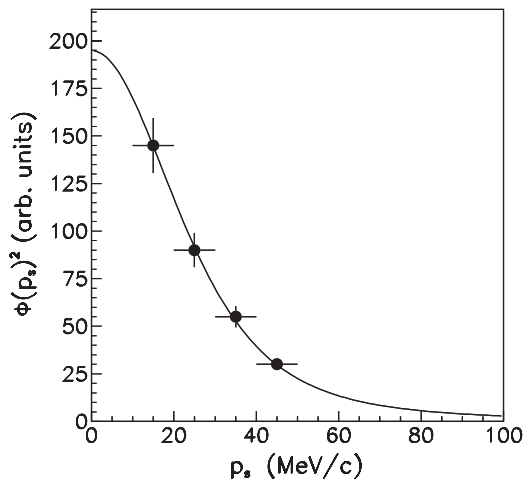

FIG. 13. Momentum distribution for p inside ^{3}He obtained as reported in the text.

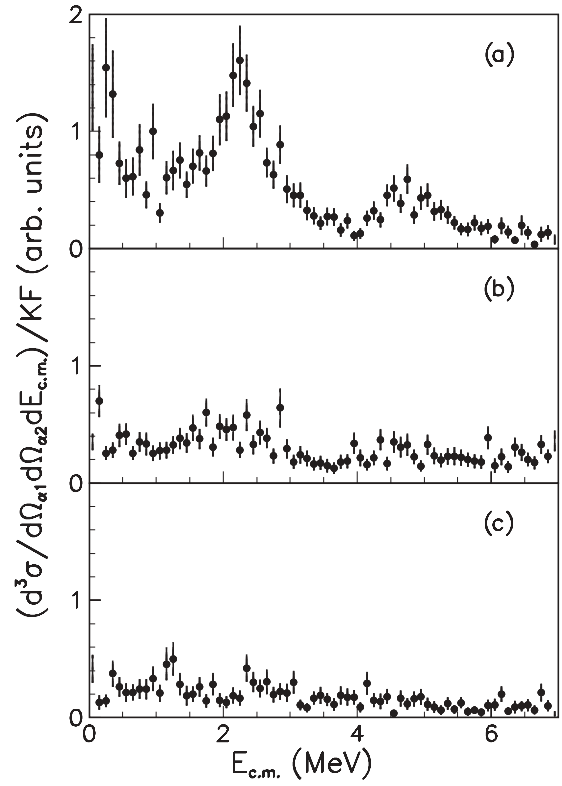

FIG. 14. Relative energy spectra for different intervals of the spectator momentum: (a) $0 \leqslant |p_s| \leqslant 20$, (b) $20 \leqslant |p_s| \leqslant 40$, (c) $50 \leqslant |p_s| \leqslant 70$ MeV/c. The decrease of the number of events as soon as one goes away from the QF condition ($p_s \approx 0$ MeV/c) is assumed as a clear evidence of the presence of the QF mechanism.

VII. THE ^{7}Li(p, α)^{4}He REACTION VIA DEUTERON AND ^{3}He BREAKUP

The ^{7}Li(p,α)^{4}He reaction was already studied with the same method extensively discussed before for ^{6}Li(d,α)^{4}He. Again a test on the TH nucleus invariance was performed and results from the deuteron and ^{3}He breakup are compared. In Ref. [18] the ^{7}Li(p,α)^{4}He was studied through the deuteron breakup while in [14] ^{3}He breakup was investigated. The two different breakup schemes are reported in Fig. 12. The same standard analysis already presented in this paper was performed for the ^{7}Li(p,α)^{4}He (as reported in [14]), studied through the ^{3}He breakup via the ^{7}Li(^{3}He,$\alpha\alpha$)^{2}H three-body reaction. Here, results with the total collected events are presented. A

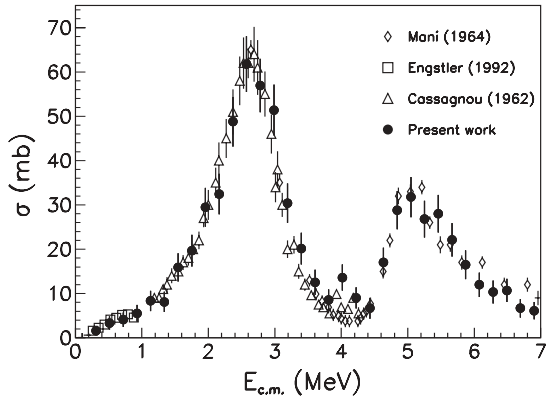

FIG. 15. Experimental ^{7}Li(p,α)^{4}He excitation function (filled circles) extracted by means of the THM using ^{3}He as Trojan horse nucleus, compared, after normalization, with direct data (open symbols) in the whole energy range.

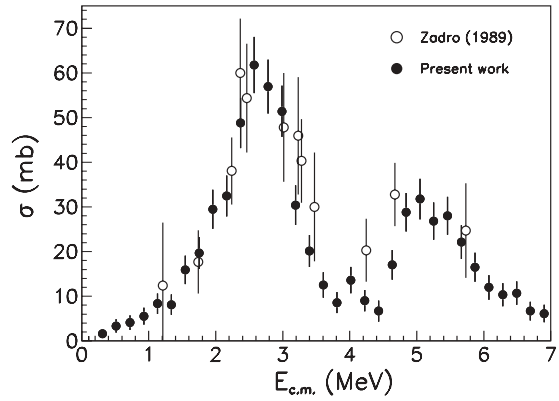

FIG. 16. Experimental ^{7}Li(p,α)^{4}He excitation function extracted by means of the THM using ^{3}He (filled circles) and deuteron (open circles [18]) as Trojan horse nucleus. The two data sets are normalized to direct data separately.

reanalysis of the experimental momentum distribution for the relative d-p motion in ^{3}He is reported in Fig. 13.

The line superimposed onto the experimental data is again the Eckart function. The very good agreement confirms that the QF mechanism is the dominant process in the selected phase space region. As in the previously examined case, only events with $|p_s| \leqslant 30$ MeV/c are used for the further analysis. In Fig. 14 the number of events projected onto the $E_{\rm cm}$ axis is shown as a function of the spectator momentum interval.

We can clearly see how going from plot (a), corresponding to events with $|p_s| \leqslant 20$ MeV/c, the number of events is greatly decreasing, until becoming negligible for conditions far away from QF ones [plot (c)]. This is taken as one of the most evident signatures of the quasifree mechanism.

In Fig. 15 the comparison of the direct and indirect excitation functions is presented in the whole explored energy range. The filled circles represent the indirect data while the direct ones [29,32,34] are reported for comparison and normalization. The agreement is evident throughout the whole energy range. The data extracted through d breakup from [18] are shown in Fig. 16 as open circles superimposed onto the filled ones. We can see that both resonances are reproduced and the agreement within the whole excitation function is very good also in this case. This gives a further validity test of the TH nucleus invariance in a different case and simultaneously above and below the Coulomb barrier. Also at lower energies the behavior is coherent with data extracted from d breakup as reported in [35].

VIII. CONCLUSION

In this paper a full investigation of the ^{6}Li(^{3}He,$\alpha\alpha$)H reaction is presented. The QF contribution is extracted and the THM applied to retrieve information on the TH nucleus invariance of the ^{6}Li(d,α)^{4}He cross section at energies above and below the Coulomb barrier. A good agreement with the direct data is achieved as well as with THM data from ^{6}Li breakup in the whole energy range. The TH particle invariance is also validated for the ^{7}Li(p,α)^{4}He cross section extracted by means of ^{3}He breakup in the ^{7}Li(^{3}He,$\alpha\alpha$)^{2}H three-body reaction. Also in this case the agreement with direct data as well as with THM data obtained from the deuteron breakup is evident (see [14]).

We conclude that the PWA is valid in both cases and that the use of a different spectator particle does not influence the THM results.

ACKNOWLEDGMENTS

This work was partially supported by Grant No. LC 07050 of the Czech MŠMT, Grant No. M10480902 of the Czech Academy, Grant No. LH1101 of the AMVIS Project, and GACR Project No. P203/10/310, and by US Department of Energy Grants No. DE-FG02-08ER41533 and No. DE-FC02-07ER41457 (UNEDF, SciDAC-2) and No. DE-FG02-93ER40773, and NSF Grant No. PHY-0852653.

[1] S. Cherubini *et al.*, Astrophys. J. **457**,855 (1996).
[2] G. Calvi *et al.*, Nucl. Phys. A **621**, 139 (1997).
[3] C. Spitaleri *et al.*, Phys. Rev. C **63**, 055801 (2001).
[4] M. Lattuada *et al.*, Astrophys. J. **562**, 1076 (2001).
[5] C. Spitaleri *et al.*, Phys.Rev. C **60**, 055802 (1999).
[6] A. Tumino *et al.*, Phys. Rev. C **67**,065803 (2003).
[7] C. Spitaleri *et al.*, Phys. Rev. C **69**, 055806 (2004).
[8] A. Tumino *et al.*, Phys. Rev. Lett. **98**, 252502 (2007).
[9] M. La Cognata *et al.*, Phys. Rev. C **76**, 065804 (2007).
[10] M. La Cognata *et al.*, Phys. Rev. C **72**, 065802 (2005).
[11] L. Lamia *et al.*, Nucl. Phys. A **787**, 309C (2007).
[12] M. L. Sergi *et al.*, Phys. Rev. C **82**, 032801 (2010).
[13] A. Musumarra *et al.*, Phys. Rev. C **64**, 068801 (2001).
[14] A. Tumino *et al.*, Eur. Phys. J. A **27**, 243 (2006).
[15] A. Tumino *et al.*, Eur. Phys. J. A **25**, 649 (2005).
[16] M. Gulino *et al.*, J. Phys. **37**, 125105 (2010).

[17] C. A. Bertulani and A. Gade, Phys. Rep. **485**, 195 (2010).
[18] M. Zadro, D. Miljanić, C. Spitaleri, G. Calvi, M. Lattuada, and F. Riggi, Phys. Rev. C **40**, 181 (1989).
[19] G. Baur, Phys. Lett. B **178**, 35 (1986).
[20] I. S. Shapiro *et al.*, Nucl. Phys. **61**, 353 (1965).
[21] N. S. Chant and P. Roos, Phys. Rev. C **15**, 57 (1977).
[22] M. La Cognata *et al.*, Phys. Rev. Lett. **101**, 152501 (2008).
[23] S. Dey *et al.*, Eur. Phys. J. A **16**, 193 (2003).
[24] I. Slaus, Nucl. Phys. A **286**, 67 (1977).
[25] R. G. Pizzone *et al.*, Phys. Rev. C **71**, 058801 (2005).
[26] R. G. Pizzone *et al.*, Phys. Rev. C **80**, 025807 (2009).
[27] A. Mukhamedzhanov *et al.*, Nucl. Phys. A **787**, 321 (2007).
[28] C. R. McClehanan and R. E. Segel, Phys. Rev. C **11**, 370 (1975).
[29] G. S. Mani *et al.*, Proc. Phys. Soc. **85**, 281 (1964).
[30] P. Paul and K. P. Lieb, Nucl. Phys **53**, 465 (1964).
[31] A. J. Elwyn, R. E. Holland, C. N. Davids, L. Meyer-Schutzmeister, J. E. Monahan, F. P. Mooring, and W. Ray Jr., Phys. Rev. C **16**, 1744 (1977).
[32] S. Engstler *et al.*, Z. Phys. **342**, 47 (1992).
[33] R. G. Pizzone *et al.*, Astron. Astrophys. **438**(3), 779 (2005).
[34] Y. Cassagnou, J. M. F. Jeronymo, G. S. Mani *et al.*, Nucl. Phys. **33**, 449 (1962).
[35] R. G. Pizzone *et al.*, Astron. Astrophys. **398**(2), 423 (2003).